Elastic constants of a Si/Ge superlattice and of bulk Si and Ge

Siqing Wei*
Department of Physics, The Ohio State University, Columbus, Ohio 43210-1106

Douglas C. Allan
Department of Physics, The Ohio State University, Columbus, Ohio 43210-1106
and Applied Process Research, SP-PR-22, Corning Inc., Corning, New York 14831

John W. Wilkins
Department of Physics, The Ohio State University, Columbus, Ohio 43210-1106
(Received 3 April 1992)

We report extensive convergence tests of the total energy of Si computed within the local-density approximation with a plane-wave basis and pseudopotentials. These convergence tests indicate that to calculate the elastic constants to about 3% relative error requires the use of 400 plane waves in the electronic structure calculation and 10 special k points to compute the density and energy. Further, we find that using the Ceperley-Alder exchange-correlation form in calculating the elastic constants obtains better agreement with the experimental results than using the Wigner form. We report the calculated lattice constants and elastic constants—bulk modulus, C_{11}, C_{12}, and C_{44}—of a "free-standing" Si/Ge ordered superlattice. For comparison, the results for bulk silicon and germanium are in excellent agreement with existing experiment and other calculations. The calculation for C_{44} reported here is unique in the sense that the "internal" atom in the diamond unit cell moves while the crystal is sheared, though previously this relaxation has been dealt with differently. The equilibrium position of the sheared crystal cannot be predicted by scaling arguments from the unstrained crystal. An "averaged elastic theory" based on bulk Si and bulk Ge predicts our computed Si/Ge lattice constant and bulk modulus surprisingly well.

I. INTRODUCTION

The local-density approximation (LDA) has proven to be an effective and useful means for studying both structural and electronic properties in many materials.[1–4] Although the method has been in existence for many years, most published calculations do not give adequate attention to the systematic study of convergence errors.[5] This is an attempt to rectify this situation in the context of calculating elastic properties.

In this paper, we report the results of convergence studies on various parameters in the method, such as the size of the plane-wave basis, the density of special k points, and the effects of different forms of exchange-correlation functions. Using recent improvements in algorithms and hardware we are able to carry the basis-set convergence to greater lengths. Comparison between Wigner and Ceperley-Alder forms of exchange-correlation potential raises the need for an improved exchange-correlation form. With the current exchange-correlation forms available, one has to choose whether to compromise the lattice constant or elastic constants: the Wigner potential gives better lattice constants while Ceperley-Alder gives better elastic constants. Next we present the theoretical predictions for the lattice and elastic constants of the "free-standing" Si/Ge superlattice (in zinc-blende structure) with comparisons to bulk Si and Ge. To ensure the accuracy, we calculate individual elastic constants according to the relationship shown in Table I. One unique aspect of this calculation is that the shear modulus (C_{44}) is obtained while allowing the atoms to relax to their equilibrium positions. The importance of this relaxation has been recognized and dealt with using other means;[6] this time this relaxation is included directly during the minimization of total energy, as it is made possible by using an iterative energy minimization scheme introduced by Car and Parrinello,[7] and later improved by Teter, Payne, and Allan,[8] which scheme will be discussed briefly in this paper.

An outline of this paper follows. In Sec. II, we describe the local-density approximation with the iterative minimization approach used in our calculation, and the details of our calculations. In Sec. III, we show the results of our convergence tests, discuss the importance of each parameter on the results, and give a realistic estimate of the errors in our results. Section IV is devoted to the results and discussion of the calculated lattice and elastic constants, where we compare our results of bulk Si and Ge with existing data, and present the results for the Si/Ge superlattice. We demonstrate the consistency of our method by comparing the elastic constants obtained from different lattice distortions discussed in the Appendix. Finally, in Sec. V, we summarize the main results of this paper.

 ©1992 The American Physical Society

TABLE I. The relationship between elastic energies, distortions, and elastic constants. The relationship between energy change (elastic energy) and distortion is shown. The choice of our distortion is to involve only one elastic constant in the energy change. The distortion is made in such a way that only the length scale of each translational vector changes. δ_i is the fractional change of the length scale in one of the three vectors with the direction indicated in the table.

Elastic constants	Unit cells	Distortions δ_1	δ_2	δ_3	Energy E/Ω
	two-atom cell (diamond)	(011)	(101)	(110)	
$B=\frac{(C_{11}+2C_{12})}{3}$		δ	δ	δ	$\frac{9}{2}B\delta^2$
	four-atom cell (001)	(110)	($\bar{1}$10)	(001)	
C_{11}		0	0	δ	$\frac{1}{2}C_{11}\delta^2$
C_{11}		2δ	2δ	$-\delta$	$\frac{9}{2}C_{11}\delta^2$
C_{44}		δ	$-\delta$	0	$2C_{44}\delta^2$
	two-atom cell (111)	($\bar{1}$10)	(01$\bar{1}$)	(111)	
C_{44}		δ	δ	-2δ	$6C_{44}\delta^2$

II. THE LOCAL-DENSITY-APPROXIMATION SCHEME AND CALCULATION METHOD

The local-density formalism[1,4,9,10] expresses the total energy of ground state as a functional of total electron charge density ρ as

$$E_{\rm tot}[\rho]=T[\rho]+E_{\rm ion}[\rho]+E_{ee}[\rho]+E_{\rm xc}[\rho]\ , \tag{1}$$

where the various terms represent the kinetic energy, the core-electron interaction, the electron-electron interaction, and the exchange-correlation energy. The density ρ is obtained as the sum of the occupied electronic states,

$$\rho(\mathbf{r})=\sum_{n\mathbf{k}}^{\rm occ}|\psi_{n\mathbf{k}}(\mathbf{r})|^2\ . \tag{2}$$

For materials with gaps in their band structures, such as insulators or semiconductors, where the occupied valence states are separated from the unoccupied conduction states, the sum in Eq. (2) runs through only those k points used to sample the Brillouin zone. In our calculation we use so-called "special" k points to conduct these Brillouin-zone summations.[11–13]

Further, the wave functions are expanded in some basis functions. In the case when the plane-wave basis is used, the wave functions $\psi_{n\mathbf{k}}$ are represented as the sums of plane waves,

$$\psi_{n\mathbf{k}}(\mathbf{r})=e^{i\mathbf{k}\cdot\mathbf{r}}\sum_{\mathbf{G}}^{N_{\rm PW}}C_{\mathbf{G},n\mathbf{k}}e^{i\mathbf{G}\cdot\mathbf{r}}\ . \tag{3}$$

The sum is cut off by the size of the basis $N_{\rm PW}$, the total number of the plane waves included.

The solution of the LDA equations for minimization of the total energy is accomplished by an iterative preconditioned conjugate gradient algorithm.[8] The use of iterative schemes to replace traditional matrix diagonalization provides a method which scales in computational effort as $N_{\rm PW}\ln N_{\rm PW}$ instead of $N_{\rm PW}^3$, which is clearly helpful as the number of plane waves $N_{\rm PW}$ grows large. The preconditioned conjugate gradient method further enhances the efficiency of the iterative minimization.

The forces on atoms are computed using the Hellmann-Feynman theorem.[14,15] The ability to move the atoms according to the calculated force is quite important in calculating the shear modulus (C_{44}) since in a shear distortion the atoms move to equilibrium positions different from the ones predicted by simple scaling of the distortion. We will discuss this in detail in Sec. IV.

Throughout our calculations, we employ the generalized norm-conserving pseudopotentials developed by Hamann[16] with the nonlocal pseudopotential being made separable using Kleinman-Bylander procedure.[17] In particular the s-wave potential is chosen to be local since that results in direct gap with nearly the same absolute error throughout the Brillouin zone for both Si and Ge, and in addition that produces a gap in bulk Ge. The Ceperley-Alder electron gas data,[18] parametrized by Teter,[19] is used for the exchange and correlation energy. Except for our systematic studies, we use a 400-plane-wave basis (corresponding to a kinetic-energy cutoff of 10 hartrees) and 10 special k points of the fcc irreducible Brillouin zone.[11–13] These k points are generalized as $\mathbf{k}\rightarrow(1+\mu)^{-1}\mathbf{k}$ in the distorted lattices, as done by Nielsen and Martin,[6] with equivalent k points added in the distorted lattices of lower symmetry. The equality of these k-point sets are verified with calculations performed using both the high- and low-symmetry sets of same structure. The systematic studies are done for the total-energy convergence versus both the size of plane-wave basis $N_{\rm PW}$ and the density of special k points, where $N_{\rm PW}$ changes from 60 to 1200, and the number of special k points from 2 to 60.

III. SYSTEMATIC CONVERGENCE STUDIES

Systematic studies of convergence are carried out for diamond structure Si. The studies are designed to test the total-energy convergence versus the k-point sampling density $N_{k\rm pt}$ and the size of plane-wave basis $N_{\rm PW}$ or kinetic-energy cutoff $E_{\rm cut}$. Also we look into the effects

TABLE II. Special k-point sets and k-point density. The relationship between special k-points and k-point density (volume or linear) is shown. The special k-point sets are usually named by the k-point numbers under fcc symmetry; the lower symmetry cells are those used in calculations of C_{11} and C_{44}, when the cell is chosen tetragonal or orthorhombic, with length scale $a_{Si}/\sqrt{2}$, $a_{Si}/\sqrt{2}$, and a_{Si}, along $(1\bar{1}0)$, (110), and (001) direction in the equilibrium. The volume density is the total number of k points within $(2\pi/a_{Si})^3$, and the linear density is the divisions in each of $(2\pi/a_{Si})$. The density increases when the unit cell size increases (since the reciprocal cell size decrease which the total number of k points remains the same).

	Number of special k-point sets				
Full diamond symmetry O_h	2	6	10	28	60
Lower symmetry with double length in (001)					
Tetragonal D_{2d}	2	8	12	36	80
Orthorhombic D_{2h}	4	16	24	72	160
Corresponding density of k points					
Volume density of k points $(2\pi/a_{Si})^3$	8	27	64	216	512
Linear density of k points $(2\pi/a_{Si})$	2	3	4	6	8

of two different exchange-correlation functional forms: Wigner[20] and Ceperley-Alder.[18]

The k-point sampling approximates the Brillouin-zone integration by a sum over some special k points[11–13]

$$\int_{BZ} f(\mathbf{k})d\mathbf{k} = \sum_{\mathbf{k}} w_{\mathbf{k}} f_{\mathbf{k}} , \tag{4}$$

where the summation is over the set of chosen k points, and w_k is the weight for each chosen k point, with $\sum_k w_k = 1$. It is important to note that the special k points are actually *uniformly spaced k points in the extended zone.* With this observation, the k-point density (whether linear or volume) is the appropriate variable for a study of the convergence over the number of k points. Table II shows the relationship between special k-point sets and the volume and linear densities of k points, measured in units of $(2\pi/a_{Si})^3$ and $(2\pi/a_{Si})$, respectively. For distorted cells with lower symmetries, Table II shows the rapidly increasing numbers of k points. The details of how a "two special k-points grid" is represented in different unit cells are shown in Table III. In this study, we concentrate on how well the integration leading to the total energy is represented by a summation over successively larger numbers of k points.

The plane-wave-basis convergence study forces on how well the incomplete basis set (with finite number of plane waves) can represent the electron wave functions of the systems we study. The number of plane waves included is determined by an energy cutoff E_{cut}, which limits the highest kinetic energy of the plane waves,

$$\tfrac{1}{2}(\mathbf{k}+\mathbf{G})^2 \le E_{cut} . \tag{5}$$

We estimate the number of plane waves within an energy cutoff E_{cut} by filling the volume of the sphere of radius $k_{cut} = \sqrt{2E_{cut}}$ with cubes with a volume of the Brillouin zone $(2\pi)^3/\Omega$,

$$N_{PW} \approx \tfrac{1}{2\Gamma}\Omega E_{cut}^{3/2} , \tag{6}$$

where Ω is the volume of the unit cell; for Si the numbers are shown in Table IV. We will study how this incomplete basis set affects the total energy, and in turn the calculated lattice and elastic constants.

A. Total-energy convergence against special k-point density

A systematic study of the total energy as a function of the linear density of k point (special k points) requires a well-defined procedure. There is no unique procedure known at this time. Ours is subject to criticism.

Our three-part procedure involves (i) assembling the

TABLE III. Example of special k points of different symmetries and unit cell size, and their density. The numbers and the coordinates of the two special k points are shown with different unit cell choices. A two-k-point set in full fcc symmetry, O_h, results in two k points in a tetragonal double cell, and four k points in an orthorhombic double cell, with a linear density of two k points per $(2\pi/a)$, and eight k points per $(2\pi/a)^3$. G is the reciprocal vector in $(2\pi/a)$ with the direction indicated.

Cells	G vectors $(2\pi/a)$			Symmetry	k point	Coordinates
Diamond	$(\bar{1}11)$	$(1\bar{1}1)$	$(11\bar{1})$	O_h	(1/4,1/4,1/4)	(1/2,1/2,1/4)
Tetragonal	$(\bar{1}10)$	(110)	(001)	D_{2d}	(0,1/4,1/4)	(1/4,1/2,1/4)
Orthorhombic	$(\bar{1}10)$	(110)	(001)	D_{2h}	(0,1/4,1/4)	(1/4,1/2,1/4)
					(1/4,0,1/4)	(1/2,1/4,1/4)
Extended zone	(100)	(010)	(001)	none	$(\pm 1/4, \pm 1/4, \pm 1/4)$	

TABLE IV. Energy cutoff E_{cut} and number of plane waves N_{PW}. The relationship between numbers of plane waves N_{PW} and energy cutoffs E_{cut} is shown for the diamond Si cell. The number of plane waves is related to the energy cutoff by the approximation $N_{PW} \approx \frac{1}{21}\Omega E_{cut}^{3/2}$, where Ω is the unit cell volume in bohr^3, E_{cut} in hartrees. For Si, $\Omega \approx 263$ bohr^3.

E_{cut} (hartrees)	3	5	10	14	20
No. of plane waves	66	141	397	656	1124

data set, (ii) devising a way of analyzing the data set, and (iii) using that analysis to estimate errors in specific properties. After this has been done for several systems, one might hope to be able to generalize the results. There is one paper of which we are aware[21] that exhibits some convergence behavior for use of special points in phonon calculations, which should bear some relation with the convergence of elastic constant calculations, but those results are for a different system and are not in a readily generalizable form. In this section and the next we use the above procedure to study the convergence of the total energy as a function of the linear density of k points N_{kpt} (see Table II) and the numbers of plane waves N_{PW} (see Table III).

1. Data set

We compute the total energy for five special k-point sets, see Table II, which correspond to a linear density of two, three, four, six, and eight k points per $(2\pi/a)$. For each of these sets, the energy is computed for five different cutoff energies E_{cut}. We thus accumulate, after 25 h on an IBM3090, twenty-five total energies: $E(E_{cut},N_{kpt})$, shown in Table V. To add five more points at the next larger k-point set would double the CPU time.

2. Analysis of data

We assume that for any given cutoff energy the total energy will converge as the density of k points (the number of special k points) approaches infinity. Unfortunately, there is no mathematical analysis as to what functional form it should have. We have tested two possible convergence forms. The first is the power law

$$E(E_{cut},N_{kpt})-E(E_{cut},\infty)=\left[\frac{N_0(E_{cut})}{N_{kpt}}\right]^{\alpha(E_{cut})}, \quad (7)$$

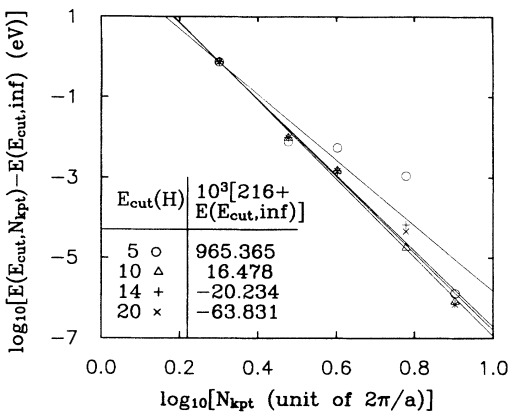

FIG. 1. Total energy convergence vs k-point density. The logarithm of the energy differences, $\log[E(E_{cut},N_{kpt})-E(E_{cut},\infty)]$, is plotted against the logarithm of N_{kpt}, the linear density of k points. $E(E_{cut},\infty)$ is obtained from a least-squares fit of our data as $\log[E(E_{cut},N_{kpt})-E(E_{cut},\infty)]=-\alpha(E_{cut})\log_{10}(N_{kpt})+\log_{10}[A(E_{cut})]$. The ○ denotes $E_{cut}=5$; △, 10; +, 14; and ×, 20 hartrees. The slopes are very close for different E_{cut} as long as E_{cut} is larger than 10 hartrees.

the other one is the logarithm

$$E(E_{cut},N_{kpt})-E(E_{cut},\infty)=\Delta E\,10^{-N_{kpt}/N_0(E_{cut})}. \quad (8)$$

Both forms have three parameters which must be fitted to only five data points for each E_{cut}—a clearly unsatisfactory situation; but this difficulty is true for almost all calculations with a finite computing budget. In Table VI, we record the values of these two sets of parameters. Even though the two $E(E_{cut},\infty)$ produced by Eqs. (7) and (8) for each E_{cut} are the same, (they differ by less than 10^{-5} meV), neither fit satisfactorily goes through all five data points, which indicates that either the actual convergence form, if one exists, might be more complicated than a simple power law or logarithmic relationship, or that our data are not in the asymptotic region where the form (7) or (8) might apply.

To characterize the fit, we plot the data and Eq. (7) in Fig. 1, we observe the following: (i) The "rate of convergence" is set by the power α. The deviation of the total energy from the estimated converged value decreases by an order of magnitude when the k-point density increases

TABLE V. Data set, the total energies of different linear k-point density, and number of plane waves $E(E_{cut},N_{kpt})$. The total energies (per atom) of a two-atom Si cell is shown with various energy cutoffs E_{cut} and k points N_{kpt}. N_{kpt} is the linear density of k points, E_{cut} is in hartrees, and the total energies are in eV. The total energy is reported here with ten effective digits as the difference between self-consistent iterations gives error in the 12th digits, while the finite size of the fast-Fourier-transform box gives error in the 11th digits.

$E_{cut}/E(N_{PW}, N_{kpt})$ \ $N_{kpt}(2\pi/a)$	2	3	4	6	8
3	−105.583 134 2	−106.262 820 3	−106.253 666 3	−106.263 003 5	−106.261 614 4
5	−106.772 855 8	−107.509 512 8	−107.511 826 3	−107.516 217 4	−107.517 320 5
10	−107.231 429 4	−107.982 055 2	−107.990 266 2	−107.991 743 5	−107.991 760 5
14	−107.249 243 5	−108.000 192 7	−108.008 662 9	−108.010 050 7	−108.010 116 1
20	−107.270 395 6	−108.022 052 5	−108.030 458 9	−108.031 870 1	−108.031 914 8

TABLE VI. Fitting parameters for convergence with k-point densities, fitted by both of power law and logarithm. The two sets of fitting parameters are shown; the two forms are as follows: The power law fit has the form $E(E_{\rm cut},N_{k\rm pt})-E(E_{\rm cut},\infty)=[N_0(E_{\rm cut})/N_{k\rm pt}]^{\alpha}(E_{\rm cut})$, and the logarithmic fit has the form $E(E_{\rm cut},N_{k\rm pt})-E(E_{\rm cut},\infty)=\Delta E(E_{\rm cut})e^{-N_{k\rm pt}/N_0(E_{\rm cut})}$. The three parameters $E(E_{\rm cut},\infty)$, $N_0(E_{\rm cut})$, and $\alpha(E_{\rm cut})$, or $E(E_{\rm cut},\infty)$, $\Delta E(E_{\rm cut})$, and $N_0(E_{\rm cut})$, are obtained through the least-squares fit to the data sets shown in Table V.

Power law \ $E_{\rm cut}$ (hartrees)	5	10	14	20
$E(\infty)$ (eV)	−107.517 321 80	−107.991 761 32	−108.010 116 78	−108.031 915 44
N_0	1.928 52	1.944 64	1.942 85	1.944 76
α	8.156 4	9.766 4	9.434 1	9.559 7
Logarithm				
$E(\infty)$ (eV)	−107.517 320 51	−107.991 760 47	−108.010 116 07	−108.031 914 74
ΔE (eV)	146.076 94	499.314 44	380.186 80	378.120 81
$N_0(2\pi/a)$	0.872 19	0.709 76	0.740 63	0.737 19

by a factor of $10^{1/\alpha}(\sim 1.3)$. Also the rate of convergence is not sensitive to $E_{\rm cut}$ for $E_{\rm cut}$ greater than 5 hartrees. (ii) The "norm" of the $N_{k\rm pt}$, $N_0(E_{\rm cut})$, is also not sensitive to $E_{\rm cut}$ for $E_{\rm cut}$ greater than 5 hartrees. (iii) The deviations of total energies from the fitted values are less 2.5 meV, for $E_{\rm cut}$ greater than 5 hartrees.

We have excluded the 3-hartrees data point from the fit because it is the only data point which does not exhibit monotonic behavior as the k-point density increases. There is no variational principle of the total energy with respect to k-point integration, so this is not disallowed, but the deviant behavior makes the fitting of a functional form more difficult. We also estimate that the convergence behavior at a 5-hartrees cutoff is not as "typical" as that of higher cutoff energies either.

3. *Error estimate*

In the calculations for lattice and elastic constants, we are interested in the energy differences between various geometries, therefore, we are more interested in the relative uncertainty rather than the absolute uncertainty. For example, when we calculate the bulk modulus, we calculate the total energies for unit cells with different lattice constants, and the total energy differences between these unit cells are the elastic energies induced by the distortions. Hence the error in the bulk modulus results from the error in the energy differences rather than the absolute error in the calculated energy for each unit cell.

We define the *relative uncertainty* as the total energy change induced by a small change in the linear density of k points connected with some physical "measurement", e.g., computing the elastic constants. We use the power-law fit [Eq. (7)] here, with all the other physical parameters remaining the same,

$$\delta E = E(E_{\rm cut},N_{k\rm pt1})-E(E_{\rm cut},N_{k\rm pt2}) = \left[\left[\frac{N_0(E_{\rm cut})}{N_{k\rm pt1}}\right]^{\alpha(E_{\rm cut})}-\left[\frac{N_0(E_{\rm cut})}{N_{k\rm pt2}}\right]^{\alpha(E_{\rm cut})}\right]. \quad (9)$$

Under hydrostatic strain where lattice constant a increases as (for Si) $a_{\rm Si}\rightarrow a_{\rm Si}(1+\delta)$, the linear density of k points increases as, since the total number of k points remains the same while the reciprocal vector length (originally $2\pi/a_{\rm Si}$) decreases, $N_{k\rm pt}\rightarrow N_{k\rm pt}(1+\delta)$. Using Eqs. (7) and (9), the relative uncertainty in the energy difference is

$$\delta E=\left[\frac{N_0(E_{\rm cut})}{N_{k\rm pt}}\right]^{\alpha(E_{\rm cut})}\left[1-\left[\frac{1}{1+\delta}\right]^{\alpha(E_{\rm cut})}\right]. \quad (10)$$

This hydrostatic distortion yields an elastic energy $E_{\rm elastic}$, hence we can define the *relative error* as the ratio of relative uncertainty δE in the energy difference, to the elastic energy $E_{\rm elastic}$:

$$\text{relative error}=\frac{\delta E}{E_{\rm elastic}}. \quad (11)$$

To estimate δE (for $E_{\rm cut}=10$ hartrees and a ten special k-points set) we use the largest volume change in our calculations, 6%, corresponding to a 2% change in the lattice constant. (We use a five-point quadratic fit with ±2%, ±1%, and 0% to obtain the equilibrium lattice constant.) Using the parameters shown in Table VI, we find $\delta E\approx 0.15$ meV. In terms of the elastic energy due to a 6% hydrostatic volume change ~75 meV, the relative error is about 0.2%. Even though this estimate is for the hydrostatic distortion, we expect that the relative error should be comparable for uniaxial and shear strains, when the other elastic constants C_{11} and C_{44} are calculated. Our evidence for this expectation is that our calculations of six and ten special k points in the unit cells with increased number of k points associated with the calculations of C_{11} and C_{44} (in cells of lower symmetry) yields same total energies as those with higher symmetry.

To compare our error estimate with other works, we consider the relative error for two special k points. Our estimate yields a relative error about 100%; from Table V we can see that the total energy changes (decreases) more than 750 meV when the linear k-point density increases from 2 to 3. Others have suggested a smaller relative error. For example, Nielsen and Martin[6] report 5% for the two special k points in their calculations for Ge. It is worth pointing out here that a two special k-point set for

the two-atom unit cell of volume $a^3/4$ has the same k-point density as a single k point (at Γ) for a 64-atom unit cell of volume $(2a)^3$. The latter is commonly used in molecular-dynamics calculations,[22] hence we believe it has the similar relative errors (100%). While this is far from a systematic treatment of k-point convergence, we can use a 10 special k-points set to ensure that the relative error is much less than 1% (0.2% in hydrostatic case).

B. Total-energy convergence against the size of the plane-wave basis

In this study, we use the same data basis established for the convergence study with k-point density. Again, we assume that for any given linear k-point density, the total energy will converge as the energy cutoff $E_{\rm cut}$ (or number of plane waves $N_{\rm PW}$, as shown in Table IV) approaches infinity. We tried both power-law and logarithmic form for this fit, power law having the form

$$E(N_{\rm PW},N_{k\rm pt})-E(\infty,N_{k\rm pt})=\left[\frac{N_0(N_{k\rm pt})}{N_{\rm PW}}\right]^{\alpha(N_{k\rm pt})}, \quad (12)$$

and logarithmic fit

$$E(E_{\rm PW},N_{k\rm pt})-E(\infty,N_{k\rm pt})=\Delta E\,10^{-N_{\rm PW}/N_0(E_{k\rm pt})}. \quad (13)$$

Both have three fitting parameters which are shown in Table VII. We stress that neither of these two fitting forms represents the data well, and the predicted converged values from these two forms are quite different: the power law gives the converged values about 10 meV lower than that obtained from logarithmic fit (Table VII). This big difference in the converged energies affects the reliability of our error estimate. In the Appendix, we present details on the nature of convergence with $N_{\rm PW}$.

Here we focus on the power-law fit shown in Fig. 2. We have the following observations. (i) The rate of convergence is set by $\alpha(N_{k\rm pt})$, which is insensitive of $N_{k\rm pt}$. We can characterize the convergence by saying that the deviation from the converged values reduced by an order of magnitude every time the number of plane waves increases by a factor of $10^{1/\alpha}$ (~ 3.5). (ii) The norm of $N_{\rm PW}$, $N_0(N_{k\rm pt})$, is likewise insensitive to $N_{k\rm pt}$.

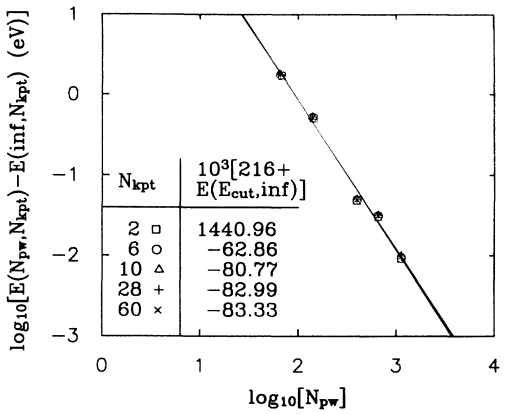

FIG. 2. Total energy convergence vs the size of plane-wave basis $N_{k\rm pt}$. The logarithm of the energy differences, $\log[E(N_{\rm PW},N_{k\rm pt})-E(\infty,N_{k\rm pt})]$, is plotted against the logarithm of $N_{\rm PW}$, the size of the plane-wave basis. $E(\infty,N_{k\rm pt})$ is obtained from a least-squares fit of our data as $\log_{10}[E(N_{\rm PW},N_{k\rm pt})-E(\infty,N_{k\rm pt})]=-\alpha(N_{k\rm pt})\log_{10}(N_{\rm PW})+\log_{10}[A(N_{k\rm pt})]$. The □ denotes two special k-point set; ○, 6; △, 10; +, 28; and ×, 60 hartrees. The slopes are almost the same for all those different k-point sets considered.

The relative error estimate is done the same way as for k-point density (discussed in Sec. III A), with the relative uncertainty for two slightly different numbers of plane waves being

$$\delta E=\left[\left[\frac{N_0(N_{k\rm pt})}{N_{\rm PW1}}\right]^{\alpha(N_{k\rm pt})}-\left[\frac{N_0(N_{k\rm pt})}{N_{\rm PW2}}\right]^{\alpha(N_{k\rm pt})}\right]. \quad (14)$$

The relative error (for a ten special k-points set and 10-hartrees energy cutoff) caused by a 6% volume change with our fitted parameters (shown in Table VII) is

TABLE VII. Fitting parameters for convergence with the size of plane-wave basis, fitted by both power law and logarithm. The two sets of fitting parameter are shown. The two fitting forms are as follows: The power law fit has the form $E(N_{\rm PW},N_{k\rm pt})-E(\infty,N_{k\rm pt})=[N_0(N_{k\rm pt})/N_{\rm PW}]^{\alpha}(N_{k\rm pt})$, and the logarithmic fit has the form $E(N_{\rm PW},N_{k\rm pt})-E(\infty,N_{k\rm pt})=\Delta E e^{-N_{\rm PW}/N_0(E_{k\rm pt})}$. The three parameters $E(\infty,N_{k\rm pt})$, $N_0(N_{k\rm pt})$, and $\alpha(N_{k\rm pt})$, or $E(\infty,N_{k\rm pt})$, $\Delta E(N_{k\rm pt})$, and $N_0(N_{k\rm pt})$, are obtained through the least-squares fit to the data sets shown in Table V.

$N_{k\rm pt}(2\pi/a)$ / Power law	2	3	4	6	8
$E(\infty)$ (eV)	−107.279 52	−108.031 43	−108.040 39	−108.041 50	−108.041 67
N_0	92.351 9	91.348 3	91.151 7	91.346 9	91.265 0
α	1.877 7	1.853 9	1.835 2	1.845 8	1.841 4
Logarithm					
$E(\infty)$ (eV)	−107.270 420	−108.022 072	−108.030 479	−108.031 893	−108.031 934
ΔE (eV)	3.182 19	3.371 196	3.371 26	3.251 31	3.366 27
N_0	231.99	227.90	228.53	231.82	228.54

$\delta E \approx 6.8$ meV, compared to the elastic energy of 75 meV. This relative uncertainty in energy differences produces a large error of 9% in our predictions for both lattice constant and bulk modulus. It is a shock that such a high energy cutoff still produces such a large relative error of 9%. But if we focus on our data shown in Table V, for the ten special k-points set, the total energy for $E_{\rm cut}=20$ hartrees is more than 40 meV lower than that of 10 hartrees. We recognize that we could be overestimating the error since the fit is not satisfactory; see the Appendix. This relative error results from the finite numbers of plane waves which change as the unit cell volume changes with a fixed energy cutoff. We expect that this error estimate for the hydrostatic distortion hold for other uniaxial distortions also. But lacking a precise formulation of how the energy should converge as, for example, the number of plane waves increases, we may be dramatically overestimating the convergence error.

C. Effects of the different exchange-correlation forms, Wigner, and Ceperley-Alder

Aside from the above convergence studies, we have also considered the effects of two different exchange-correlation forms—Wigner versus Ceperley-Alder–on the bulk modulus and the lattice constants for all three systems we studied: bulk Si, Ge, and superlattice Si_1/Ge_1. We find that the Wigner form gives a larger lattice constant (better agreement with experiment) and Ceperley-Alder gives a larger bulk modulus (better agreement with experiment). This is true for all three systems, as summarized by two observations. (i) When we compare the exchange-correlation n energies around the electronic density of Si or Ge, ($r_s \approx 2$), we find that Wigner's $V_{\rm xc}^{W}$ is less attractive than Ceperley-Alder's $V_{\rm xc}^{\rm CA}$; this decreased attraction explains why we get larger lattice constant with Wigner's exchange-correlation potential. (ii) When we compare the bulk moduli, we find that the exchange-correlation contribution to the bulk modulus is negative around $r_s=2$, and it is 70 kbar more negative using the Wigner form than using Ceperley-Alder; this larger negative contribution explains the smaller bulk modulus resulted by using Wigner form. Hence a smaller bulk modulus resulted from the Wigner form. These observations, well known in the electronic structure community,[23] once again point to the need for an improved exchange-correlation form.

D. Conclusions

The Wigner exchange-correlation potential gives better lattice constants while Ceperley-Alder gives better elastic constants. We choose the Ceperley-Alder potential, since this work is more focused on the elastic constants than on the structural properties. We have introduced the "relative error" as a measure of convergence and error estimate. We find that a 10 special k-point set will virtually eliminate the error (0.2%) due to finite sampling k point in Brillouin zone, but that even a large (10 hartrees) energy cutoff still yields an error of 9%.

IV. THE CALCULATED RESULTS FOR Si, Ge, AND Si/Ge

The elastic constants are calculated through finite differences, with quadratic fits for five to seven data points (five points for bulk modulus, lattice constant, and C_{11}; seven points for C_{44}). According to Nye,[24] the total energy change per volume due to the elastic distortions is

$$\frac{\Delta E_{\rm tot}}{\Omega}=\tfrac{1}{2}C_{11}(e_1^2+e_2^2+e_3^2)+C_{12}(e_1e_2+e_2e_3+e_3e_1)+\tfrac{1}{2}C_{44}(e_4^2+e_5^2+e_6^2)\ , \tag{15}$$

where Ω is the supercell volume, and $C_{11,12,44}$ are the elastic constants, and $e_{1,\ldots,6}$ is the six-dimensional strain "vector."

There are two aspects in this work we want to emphasize: (i) The distortions are chosen to involve only one single elastic constant in the total energy change for a given geometry. With this choice of strain, we can rewrite Eq. (15) in the following form:

$$\frac{\Delta E_{\rm tot}}{\Omega}=KC_{ij}e_k^2\ , \tag{16}$$

where the C_{ij} is the elastic constant we wish to calculate, e_k is the strain due to the chosen distortion, and the K is just a proportionality constant; see Table I. (ii) This time atomic relaxation is directly included when unit cell is under a shear distortion, though the effect of this relaxation was included by Nielsen and Martin[6] using a different approach. The relaxation $\mathbf{d}$ of the atom in diamond structure Si and Ge (zinc-blende Si/Ge) under shear distortion $e_{4,5,6}$ in Cartesian coordinates is expressed as

$$\mathbf{d}=\zeta\frac{a}{4}(e_4,e_5,e_6)\ , \tag{17}$$

where a is the lattice constant, $e_{4,5,6}$ are the shear strains, and ζ is the internal shift parameter. Our results show that this relaxation reduces the C_{44}^0 obtained from nonrelaxed calculation by about 25% to agree with the experimental value, for both bulk Si and Ge.

A. Si and Ge provide test of method

Table VIII shows our calculated results together with the experiment[25–29] and other LDA calculations[6] for bulk Si and Ge. The slight differences between our result and that of Nielsen and Martin are the (i) different exchange-correlation forms used in calculations for Si (they used Wigner form while we use Ceperley-Alder form); (ii) different special k-point sets for Ge (they used two special k points while we use ten special k points).

Comparing our results to the experiment, we can see that, except for ζ,[30] our results for both Si and Ge agree well (no more than 3% difference). The good agreement between our results and experimental data prove that our method is accurate, and establishes the solid foundation for predicting the properties of new materials, in our case, the zinc-blende Si_1/Ge_1 superlattice.

The large discrepancy between our calculated ζ and

the experimental values is believed to be experimental error.[30,31] In part, this belief is supported by our estimate of ζ using empirical two- and three-body potentials for Si.[31] Consider a distortion η in the (111) direction; the elements of strain tensor μ are

$$\mu_{ij}=\tfrac{1}{3}\eta \ . \tag{18}$$

Using Eq. (17) and the definition of strain tensor the relaxed atomic position is

$$\mathbf{r}'=(\mathbf{1}+\mu)\mathbf{r}+\mathbf{d} \ , \tag{19}$$

where $\mathbf{r}$ is chosen as $(a/4)(1,1,1)$ in the undistorted cell. With both μ and ζ, we can calculate the changes of the bond lengths and bond angles of the relaxed atom to its four nearest neighbors. The change in bond length l along the (111) direction dl_1 is $(1-\zeta)\eta l$, while the change of the other bond lengths dl_2, dl_3, and dl_4 in the directions of $(\bar{1}\,\bar{1}1)$, $(\bar{1}1\bar{1})$, and $(1\bar{1}\,\bar{1})$ are the same and equal to $(1+3\zeta)\eta l/9$. The three bond angles $d\theta_{102}$, $d\theta_{103}$, and $d\theta_{104}$ involving the (111) bond are changed by the same amount of $\sqrt{8}(1+3\zeta)/9$, while the other three bond angles $d\theta_{203}$, $d\theta_{204}$, and $d\theta_{304}$ have a change of the same magnitude but opposite sign. The numbers in the subscripts indicate the nearest neighbors of the relaxed atom (with 0 being the position of the central atom). The equilibrium bond angle $\theta=\cos^{-1}(-\frac{1}{3})$.

To estimate the optimal ζ, we assume a simple elastic energy form of a quadratic function of bond length (two-body) and bond angle (three-body)

$$\begin{aligned}E(dl,d\theta)&=A\sum_i\left[\frac{dl_i}{l}\right]^2+B\sum_j\left[\frac{d\theta_j}{\theta}\right]^2\\&=\eta^2A[(1-\zeta)^2+\tfrac{3}{81}(1+3\zeta)^2]\\&\quad+\eta^2B\left[\frac{16}{27}\frac{1}{\theta^2}(1+3\zeta)^2\right] .\end{aligned} \tag{20}$$

where A and B are force constants. Minimizing $E(dl,d\theta)/(\eta)^2$, we have the optimal ζ,

$$\zeta=\frac{2}{3}\left[\frac{1-(2/\theta^2)(B/A)}{1+(4/\theta^2)(B/A)}\right] . \tag{21}$$

In order to evaluate the ratio of (B/A), we use the data from the empirical two- and three-body potential developed by Stillinger and Weber.[31] Expanding their potential around equilibrium bond length and bond angle, we find $B/A=0.14998$. Substituting this ratio into Eq. (21) yields $\zeta=0.5255$, which agrees with our calculated result for Si (0.53–0.56).[30]

B. Results for Si/Ge superlattice

As a first attempt at characterizing our results for the superlattice (zinc-blende Si_1/Ge_1) (Table VIII), we compare with the corresponding values of bulk Si and Ge. Note that the superlattice results lie intermediate between, as common sense would suggest.[32] For a closer look, we compare our LDA results with "elastic theory"

TABLE VIII. Lattice constants a, bulk modular B, elastic constants C_{ij} of Si, Ge, are Si/Ge. Lattice constant in a_0 elastic constants in Mbar (100 GPa). C_{12} deduced from B and C_{11} via $C_{12}=\frac{1}{2}(3B-C_{11})$. Unrelaxed elastic constant C_{44}^0, internal relaxation parameters ζ.

	a			B			C_{11}			C_{12}		
	Si	Ge	Si/Ge	Si	Ge	Si/Ge	Si	Ge	Si/Ge	Si	Ge	Si/Ge
NM[a]	10.21	10.57		0.93	0.72		1.59	1.30		0.61	0.45	
This work	10.17	10.51	10.32	0.97	0.77	0.88	1.64[b]	1.34[b]	1.50[b]	0.64	0.49	0.57
This work							1.62[c]	1.32[c]	1.51[c]			
Expt.[f]	10.27[g]	10.68[g]		0.99	0.77		1.68	1.32		0.65	0.49	
	a			C_{44}^0			C_{44}			ζ		
	Si	Ge	Si/Ge	Si	Ge	Si/Ge	Si	Ge	Si/Ge	Si	Ge	Si/Ge
NM[a]	10.21	10.57		1.11	0.77		0.85	0.68		0.53	0.44	
This work (110)[d]	10.17	10.51	10.32	1.10	0.89	0.99	0.80	0.69	0.73	0.56	0.57	0.59
This work (111)[e]							0.77	0.68	0.75	0.53	0.50	0.51
Expt.[f]	10.27[g]	10.68[g]					0.80	0.68		0.73[h]	0.72[h]	
Expt.										0.64[i]	0.64[i]	

[a]O. H. Nielsen and Richard Martin, Phys. Rev. B **32**, 3797 (1985).
[b]Volume changed, distortion in (001) (see Table I).
[c]Volume unchanged, compress in (001), expand in both (110) and $(\bar{1}10)$ (see Table I).
[d]Expand in (110) and compress in $(\bar{1}10)$ (see Table I).
[e]Distortion in (111) direction (see Table I).
[f]H. J. McSkimin, J. Appl. Phys. **24**, 988 (1953); **35**, 3312 (1964), except otherwise indicated.
[g]J. Donohue, *The Structures of the Elements* (Wiley, New York, 1974).
[h]H. d'Amour *et al.*, J. Appl. Crystallogr. **15**, 148 (1982); C. S. G. Cousins *et al.*, *ibid.* **15**, 154 (1982).
[i]A. Segmuller and H. R. Neyer, Phys. Kondens. Materie. **4**, 63 (1970).

predictions on lattice constant and bulk modulus.

What we mean by "elastic theory" is this: we require the compound (Si_1/Ge_1 ordered alloy) to have minimum elastic energy with each atomic species retaining its original lattice constant and bulk modulus. In the case of Si_1/Ge_1, the elastic energy per volume is

$$\frac{E[(a_{Si/Ge}-a_{Si}),(a_{Si/Ge}-a_{Ge})]}{\Omega} = \frac{9}{4}B_{Si}\left[\frac{(a_{Si/Ge}-a_{Si})}{a_{Si}}\right]^2 + \frac{9}{4}B_{Ge}\left[\frac{(a_{Si/Ge}-a_{Ge})}{a_{Ge}}\right]^2, \quad (22)$$

where $a_{Si/Ge}$ is the lattice constant of Si_1/Ge_1. Minimizing the elastic energy respect to $a_{Si/Ge}$, we have

$$a_{Si/Ge} = \left[\frac{B_{Si}}{a_{Si}}+\frac{B_{Ge}}{a_{Ge}}\right] \Big/ \left[\frac{B_{Si}}{a_{Si}^2}+\frac{B_{Ge}}{a_{Ge}^2}\right]. \quad (23)$$

By the same token, we can get the elastic theory prediction of bulk modulus for $Si_1/Ge/1$,

$$B_{Si/Ge} = \frac{1}{2}\left[B_{Si}\left[\frac{a_{Si/Ge}}{a_{Si}}\right]^2 + B_{Ge}\left[\frac{a_{Si/Ge}}{a_{Ge}}\right]^2\right]. \quad (24)$$

The LDA results for bulk Si and Ge can then "predict" values for Si_1/Ge_1. See Table IX. The difference between the LDA calculated property and the one predicted by elastic theory is less than 0.1% for the lattice constant and 1% for the bulk modulus. Such close agreement is unexpected since this mean-field elastic theory would be expected to valid at most in the long-wavelength limit.[32]

To sum up, (i) we have developed a scheme to calculate each elastic constant separately, which eliminates the error in the fitting process; (ii) we allow atoms to relax during the calculations of shear modulus C_{44} and the relaxation reduces the calculated value by 25% to agree with the experiment; (iii) this is a prediction for the elastic properties of the as yet unsynthesized Si_1/Ge_1. We argue that the accuracy of these predictions are supported by the agreement between our results for bulk Si and Ge with both previous theory and experimental data.

TABLE IX. "Elastic theory" (ET) predictions of lattice constant and bulk modulus for Si_1/Ge_1. The elastic theory prediction of the Si_1/Ge_1 lattice constant and bulk modulus is shown. The lattice constants are in bohr; bulk moduli in Mbar (=100 GPa). The predictions are based on our LDA results for bulk Si and Ge (lattice constant and bulk modulus), and the comparison is made with the LDA results of Si_1/Ge_1. The worse agreement seen on bulk modulus is due to the limited number of digits reported; actual agreement is within 0.4%.

	Si (LDA)	Ge (LDA)	Si/Ge (ET)	Si/Ge (LDA)
a	10.17	10.51	10.33	10.32
B	0.97	0.77	0.87	0.88

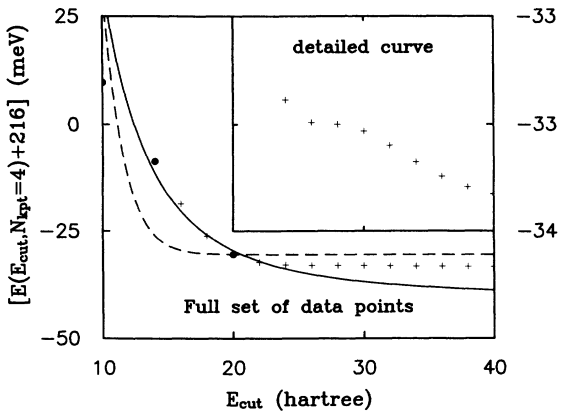

FIG. 3. Total energy vs energy cutoff E_{cut}. The total energy, in eV, is plotted against the energy cutoff E_{cut}, in hartrees. The inset shows a "step" for E_{cut} between 25 and 40. This step in the convergence makes it impossible to fit the data with any simple form. The solid curve is the fit of the total energy by power law, and the dashed curve is by logarithm, the dots are the data points used for the fit (see Table VII); note that the two lowest data points, at $E_{cut}=3$ and 5, are not shown.

V. CONCLUSIONS

We have reported convergence studies of total energy versus various aspects in the local-density approximation calculations, such as a function of the size of the plane-wave basis and of the density of the special k-point grids. The results show that the incompleteness of the plane-wave basis is the major source of error in these calculations; even with a large energy cutoff of 10 hartrees (400

TABLE X. Total energy of ten special k points for various energy cutoffs. The calculated total energy for the two-atom Si cell is shown here. The total energy is reported with ten effective digits as the error in our self-consistant shows in the 12th digits and finite fast-Fourier-transform box shows in the 11th digits. E_{cut} is in hartrees, total energy is in eV, and N_{PW} is the average number of the plane waves for ten special k points used in the calculations.

E_{cut} (hartrees)	Total energy (eV)	N_{PW}
3	−106.253 666 3	65.06
5	−107.511 826 3	140.16
10	−107.990 266 2	397.75
14	−108.008 662 9	658.0
16	−108.018 612 7	804.09
18	−108.026 144 5	960.5
20	−108.030 458 9	1125.0
22	−108.032 325 5	1298.9
24	−108.032 886 0	1479.0
26	−108.032 990 6	1666.8
28	−108.032 999 7	1864.1
30	−108.033 032 2	2065.19
32	−108.033 098 4	2274.75
34	−108.033 176 8	2491.44
36	−108.033 244 9	2716.56
38	−108.033 294 7	2944.12
40	−108.033 327 6	3181.59

plane waves), there is still about 9% relative error in the lattice and elastic constants. The finite density of k points accounts for less error, only 0.2% for a ten special k-point set. These convergence studies point to a way to realistic error estimation in the future work. But we could stress that we expect the error due to the k-point set to increase as the energy gap decreases.

One unique aspect of our elastic constant calculation is that we actually allow the atoms to relax during our calculation. This relaxation produces agreement between theory and experiment for the shear modulus C_{44}. As a first step in our effort to understand Si/Ge superlattices, we have presented the results on Si_1/Ge_1; these results are validated by the agreement between our results and experiment on bulk Si and Ge.

In conclusion, we have (i) an efficient and accurate method to determine the ground-state properties of Si/Ge systems; and (ii) a realistic error estimation, and these methods may be used in more complicated Si/Ge systems.

ACKNOWLEDGMENTS

We acknowledge the invaluable help and discussion of Zachary Levine. This work was supported by the Department of Energy-Basic Energy Science, Division of Materials Sciences. The computation was performed through the support of Cornell National Supercomputer Facility and we thank the staff members at Cornell Theory Center for their help.

APPENDIX: TOTAL ENERGY AND ENERGY CUTOFF (SIZE OF PLANE-WAVE BASIS)

Since, as pointed out in Sec. III B, neither a power law nor a logarithmic fit is satisfactory, we decided to look more carefully at how the total energy changes as the energy cutoff increases. Table X shows the total energies of ten special k points with E_{cut} from 10 to 40 hartrees with an interval of 2 hartrees. The total energy is plotted against the energy cutoff in Fig. 3; we can see that in the full scale plot, the total energy decreases as E_{cut} increases. But in the inset for E_{cut} between 25 and 40, we see that the convergence is not smooth: the rate of converge slows down, and then speeds up and slows down again. This change in convergence pace makes it impossible to fit the data set with any simple form, and results in a poor fit, as discussed in Sec. III B.

*Permanent address: School of Physics, Georgia Institute of Technology, Atlanta, GA 30332-0430.

[1]R. O. Jones and O. Gunnarsson, Rev. Mod. Phys. **61**, 689 (1989), and references therein.
[2]W. Pickett, Comput. Phys. Rep. **9**, 115 (1989).
[3]J. D. Joannopoulos, in *Physics of Disordered Materials,* edited by D. Adler, H. Fritsche, and S. R. Ovshinsky (Plenum, New York, 1985), p. 19.
[4]U. von Barth, in *Many-Body Phenomena at Surfaces,* edited by D. Langreth and H. Suhl (Academic, New York, 1984), p. 3.
[5]A counterexample to prevailing practice, where basis-set convergence data actually are given, is found in M. T. Yin and M. L. Cohen, Phys. Rev. B **26**, 3259 (1982), Table III; and **26**, 5668 (1982), Table XI.
[6]O. H. Nielsen and R. Martin, Phys. Rev. B **32**, 3797 (1985).
[7]R. Car and M. Parrinello, Phys. Rev. Lett. **55**, 2471 (1985); **60**, 204 (1988).
[8]M. P. Teter, M. C. Payne, and D. C. Allan, Phys. Rev. B **40**, 12 255 (1989).
[9]P. Hohenberg and W. Kohn, Phys. Rev. **136**, B864 (1964).
[10]W. Kohn and L. J. Sham, Phys. Rev. **140**, A1133 (1965).
[11]D. J. Chadi and M. L. Cohen, Phys. Rev. B **8**, 5747 (1973).
[12]H. J. Monkhorst and D. J. Pack, Phys. Rev. B **13**, 5188 (1976).
[13]R. A. Evarestov and V. P. Smirnov, Phys. Status Solidi B **119**, 9 (1983).
[14]H. Hellmann, *Einführung in die Quantenchemie* (Deuticke, Leipzig, 1937), pp. 61 and 285.
[15]R. P. Feynman, Phys. Rev. **56**, 340 (1939).
[16]D. R. Hamann, Phys. Rev. B **40**, 2980 (1989).
[17]L. Kleinman and M. Bylander, Phys. Rev. Lett. **48**, 1425 (1982).
[18]D. M. Ceperley and B. J. Alder, Phys. Rev. Lett. **45**, 566, (1980).
[19]M. P. Teter (private communication). This is a Padé approximant to the data of Ceperley and Alder, which therefore has continuous derivatives unlike the Perdew-Zunger parametrization.
[20]E. Wigner, Phys. Rev. **46**, 1002 (1934); D. Pines, *Elementary Excitations in Solids* (Benjamin, New York, 1963), p. 94.
[21]D. Singh and Y. P. Varshni, Phys. Rev. B **30**, 6917 (1984).
[22]F. Buda, R. Car, and M. Parrinello, Phys. Rev. Lett. **41**, 1680 (1990).
[23]R. O. Jones and O. Gunnarsson, Rev. Mod. Phys. **61**, 698 (1989).
[24]J. F. Nye, *Physical Properties of Crystals* (Oxford University Press, London, 1969), p. 131.
[25]H. dÁmour *et al.*, J. Appl. Crystallogr. **15**, 148 (1982).
[26]C. S. G. Cousins *et al.*, J. Appl. Crystallogr. **15**, 154 (1982).
[27]A. Segmuller and H. R. Neyer, Phys. Kondens. Materie. **4**, 63 (1970).
[28]J. Donohue, *The Structures of the Elements* (Wiley, New York, 1974).
[29]H. J. McSkimin, J. Appl. Phys. **24**, 988 (1953); **35**, 3312 (1964).
[30]Recent comments of C. S. G. Cousins indicate that the earlier experiment results for ζ might be overestimated. In Eq. (21), if we only consider the two-body potential ($B=0$) $\zeta=\frac{2}{3}$, this leads to all four bond lengths being the same; if we only consider the three-body potential ($A=0$) $\zeta=-\frac{1}{3}$, this leads to all six bond angles being the same (unchanged). One should expect that ζ should be between $-\frac{1}{3}$ and $\frac{2}{3}$ for normal diamond structured materials.
[31]Stillinger and Weber, Phys. Rev. B **32**, 5262 (1985).
[32]John R. Dutcher *et al.*, Phys. Rev. Lett. **65**, 1231 (1990).